Chemical Sensitivity of Valence-to-core X-ray Emission Spectroscopy due to the Ligand and the Oxidation State: A Computational Study on Cu-SSZ-13 with Multiple H_2O and NH_3 Adsorption

Renqin Zhang[a]†, Hui Li[a,b]†, Jean-Sabin McEwen[a,c,d,e*]

[a]*The Gene and Linda Voiland School of Chemical Engineering and Bioengineering, Washington State University, Pullman, WA 99164*

[b]*College of Materials Science and Engineering, Taiyuan University of Technology, Taiyuan, China 030024*

[c]*Department of Physics and Astronomy, Washington State University, Pullman, WA 99164*

[d]*Department of Chemistry, Washington State University, Pullman, WA 99164*

[e]*Institute for Integrated Catalysis, Pacific Northwest National Laboratory, Richland, WA, 99352*

Abstract

Valence-to-core X-ray emission spectroscopy (vtc-XES) is a powerful experimental tool that can overcome the sensitivity limitations of X-ray absorption near edge structure (XANES) measurements with regard to the ligand identification. To further elucidate the sensitivity of this experimental technique, the corresponding emission spectra of a Cu cation when exchanged within a chabazite structure (Cu-SSZ-13) was calculated from first principles. By comparing vtc-XES spectra of H_2O and NH_3 adsorbed on Cu^+ (or Cu^{2+}) cations, we find a blue shift for the kβ" lines from a Cu-O to a Cu-N ligation. In addition, the adsorption of NH_3 results in a stronger $k\beta_{2,5}$ line intensity than the corresponding one for H_2O. Therefore, one can discriminate the adsorption of H_2O or NH_3 by the different vtc-XES emission lines of Cu-O and Cu-N. By scanning the vtc-XES of multiple H_2O and NH_3 adsorbed Cu-SSZ-13 structures, we find a shift in the energy of the kβ′′ line between H_2O and NH_3 adsorbed conformations, which increases by increasing the population of Cu-ligand bonds for both the Cu^+ and Cu^{2+} cations. By analyzing the partial density of states (PDOS) for these structures, the kβ" emission line results from a N 2*s* to Cu 1*s* transition while the $k\beta_{2,5}$ emission line is generated from the transition going from a mixed N 2*p*, Cu 3*d* and 4*p* states to a Cu 1*s* core hole, where the Cu 4*p* state plays a key role in this transition. Further PDOS analysis shows the chemical sensitivity of vtc-XES since ligand environment is intrinsically determined by the different potential binding energies of ligand 2s states. Finally, we compare our computed XES results to the measured XES of several reference compounds, which seem to suggest a different assignment than what was suggested in the literature. As such, the vtc-XES spectrum is a complementary tool to the XANES and is well-suited for uncovering the state of the active site and the nearest neighbor environment of Cu ions in Cu-SSZ-13 during the selective catalytic reduction of NO or, more generally, of metal ions in a working catalysts.

†Contribute equally; *Corresponding author: js.mcewen@wsu.edu

1. Introduction

A number of reports on copper-exchanged SSZ-13 (Cu-SSZ-13), claim that it is more active and selective toward the formation of N_2 in the selective catalytic reduction (SCR) of NO with NH_3 as compared to Cu-ZSM-5 and Cu-beta.[1] Also, it was found that Cu-SSZ-13 is more hydrothermally stable than the Cu-Y, Cu-ZSM-5, and Cu-beta zeolites and that this is likely due to the smaller cavity dimensions that make up the CHA structure.[2] The spectroscopic properties[3-5] of Cu-SSZ-13 have attracted significant attention due to their potential for uncovering chemical bonding and electronic structure relationships as well as the mechanism of SCR on Cu ions,[6, 7] which could further support the design of new catalysts.

X-ray absorption spectroscopy (XAS) is a versatile tool that is sensitive to the oxidation state and the local structure of the probed atoms.[8] Cu K-edge X-ray absorption near edge structure (XANES) spectra have been widely used to determine the oxidation state and local structure of Cu cations in different species.[6, 7, 9, 10] However, as pointed out by Matthias Bauer,[11] an XAS analysis suffers from a lack of sensitivity of the ligands that coordinate to the metal ions. This difficulty of ligand identification gives rise to a serious hindrance in our ability to uncover the underlying mechanism in the SCR of NO_x with NH_3 with regard the role of each gaseous component in the reaction and the structure of principal intermediates species. This limitation could be overcome by using valence-to-core X-ray emission spectroscopy (vtc-XES), which is used for the characterization of the valence electronic levels.[12-14] Under standard SCR conditions, the XANES spectra of the Cu cations are found to be independent of the Si/Al ratio, although the Cu-complexes are $Cu^{2+}(NH_3)_4$ and $[Cu^{2+}(OH^-)]^+(NH_3)_3$ for low and high Si/Al ratios, respectively.[6] XANES cannot distinguish the species of $Cu^{2+}(NH_3)_4$ and $[Cu^{2+}(OH^-)]^+(NH_3)_3$. Using vtc-XES, it is possible to distinguish oxygen or nitrogen ligation of the Cu active sites.[13, 14] This technique provides more information concerning the valence electron orbitals near the Fermi level, which are formed by the interaction between the metal and ligand orbitals. Consequently, vtc-XES is highly sensitive to the ligands and provides complementary information to an XAS analysis. For example, it was found that the temperature strongly influences the local structures of Cu ions during SCR by combining XANES and XES techniques.[13] The aforementioned analysis concluded that low-temperature SCR is characterized by balanced populations of Cu^+/Cu^{2+} sites and dominated by mobile NH_3-solvated Cu-species while the largely dominant Cu-species are framework-coordinated Cu^{2+} sites under high-temperature SCR.[13, 15]

Thanks to the development of density functional theory and more powerful computational resources, vtc-XES spectra can be modeled, providing further insights into spectroscopic properties at the atomic and electronic level.[16-19] Grunwaldt and coworkers studied the vtc-XES of

Cu-SSZ-13 under different conditions and found different feature peaks in vtc-XES spectra for Cu-SSZ-13 samples with and without NH_3 in the feed.[20] The difference is attributed to a N atom in the coordination sphere of Cu ions. Computational vtc-XES based on DFT calculations of cluster models with and without NH_3 confirmed this experimental finding.[20] However, further analysis at an electronic level is missing. Lamberti and coworkers also employed several techniques combined with a computational analysis of vtc-XES to find that the dominant structural components of Cu-SSZ-13 upon O_2-activation and He-activation are $[CuOH]^+$ and bare Cu^+ cations, respectively.[21] Computational spectroscopic studies are advantageous due to their ability to aid theoretical interpretations on experimental results and, to some extent, propose new hypotheses that can be verified by additional experiments.[3, 21] As part of our continuing efforts toward understanding the spectroscopic properties of Cu-SSZ-13, we studied vtc-XES of the Cu cations in Cu-SSZ-13 under different conditions. We employed Cu-SSZ-13 models with periodic boundary conditions and excited a 1s core electron to generate vtc-XES spectra. In this contribution, we will investigate the sensitivity of vtc-XES on ligation, population of adsorbed molecules, and oxidation state for Cu cations in Cu-SSZ-13. We will present our insight into our ability to identify ligand environments of Cu cations using vtc-XES by performing a density of state (DOS) analysis when the 1s core electron is excited. The use of DFT surely represents a significant step forward toward a more robust spectroscopic interpretation.

2. Computational details

DFT calculations for the energetics were performed with the Vienna *Ab initio* Simulation Package (VASP).[22, 23] The projector augmented-wave (PAW)[24, 25] method and the generalized-gradient approximation (GGA), using the PW91 functional,[26] were employed for the treatment of the electron-ion interactions and the exchange-correlation effects, respectively. With PAW potentials, VASP combines the accuracy of all-electron methods with the computational efficiency of plane-wave approaches. The total energy convergence threshold was set to 10^{-8} eV and the geometries were considered to be fully relaxed when the forces were less than 0.01 eV/Å. A 400 eV plane-wave cutoff and a single Γ-point sampling of the Brillouin zone were used for the optimization calculations. A rhombohedral unit cell of SSZ-13 was used in this study. More detailed information about the structure of the rhombohedral unit cell can be found in our previous work.[4]

The Cu^+/Cu^{2+} redox reaction plays an important role in the mechanism of the SCR reaction on Cu-SSZ-13.[6, 7, 27-30] In the rhombohedral unit cell, charge deficiencies are generated upon replacement of Si atoms by Al atoms. Up to 2 Si atoms can be substituted by Al atoms within our system, which can result in sites containing 1 or 2 charge deficiencies. Cu cations are then used to

compensate such insufficiencies, which determine their formal oxidation states, which can be +1 or +2. The corresponding Cu-SSZ-13 zeolites are denoted as ZCu (1Al) and Z_2Cu (2Al), which represent Cu-SSZ-13 with high and low Si/Al ratios, respectively. Cu^{2+} cations in Z_2Cu could be reduced and the new charge deficiency compensated by an H^+ cation. The corresponding conformation is labeled as HZ_2Cu. For a ZCu sample, a Cu^+ cation could be oxidized to Cu^{2+} by forming $[Cu^{2+}(OH^-)]^+$, denoted as ZCuOH. The $[Cu^{2+}(OH^-)]^+$ conformation has been reported via from a number of different techniques.[4, 30-32] The Cu^+/Cu^{2+} redox reaction happens in 1Al and 2Al samples via ZCu ⇔ ZCuOH and HZ_2Cu ⇔ Z_2Cu, respectively. Paolucci et al. demonstrated that 1Al and 2Al samples exhibit similar turnover rates, apparent activation energies, and apparent reaction orders under standard SCR conditions.[6] The local structures of the Cu cation for ZCu, HZ_2Cu, Z_2Cu and ZCuOH configurations are shown in Figure 1. In this contribution, the vtc-XES of Cu cations in ZCu, HZ_2Cu, Z_2Cu and ZCuOH when bonded to multiple NH_3 and H_2O, with the molecular number ranging from 1 to 6, are generated through DFT calculations. Optimized structures of multiple NH_3 and H_2O (n=1 to 6) adsorbed on Cu-SSZ-13 are shown in Figure S1 of the Supporting Information. Each conformation is denoted as molecule_n_Cu-SSZ-13. For example, NH_3_1_ZCu is for 1 NH_3 adsorbed within the ZCu conformation.

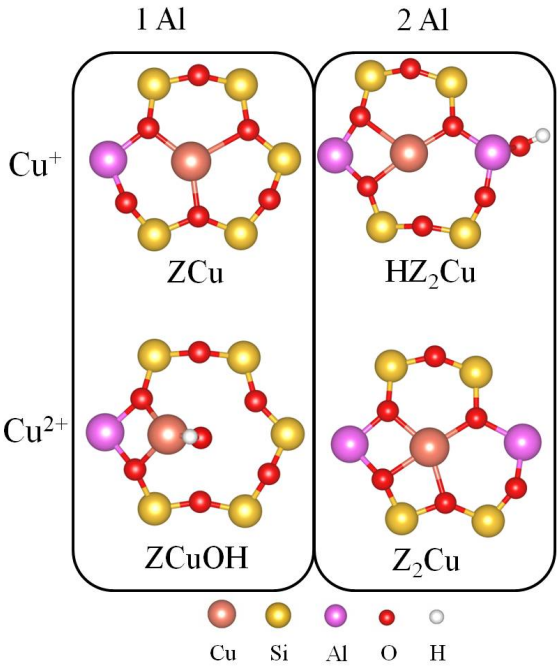

Figure 1. Local structures of a Cu cation in ZCu, HZ_2Cu, Z_2Cu and ZCuOH conformations. The 1Al and 2Al notation denotes 1 or 2 Al atoms are within the rhombohedral unit cell of Cu-SSZ-13, respectively. The legend for the atoms is shown in the bottom.

The calculations of the vtc-XES spectra, the corresponding projected density of states

(PDOS) analyses, and the orbital calculations for Cu cations in Cu-SSZ-13 were performed using the CASTEP code.[33] Ultrasoft pseudopotentials were generated on the fly[34] where one electron was excited from the 1s core level when performing core-hole calculations. Energy cutoffs of 550 eV and k-point grids of (5×5×5) were used. Spectral broadening due to instrumental smearing was employed using the Gaussian method, using a value of 0.6 eV and lifetime broadening was applied with a value of 1.55 eV.[34] In order to obtain accurate PDOS for Cu, N and O, k-point grids of (5×5×5) were still used. The PDOS from the ground state calculation is quite different for the PDOS from the final state where the Cu 1s electron is excited.[4] Further, several works demonstrate that the XANES features correlate well with the DOS of the excited state.[4, 5, 35] As a result, we will be comparing the PDOS in the final (excited) state to analyze our computed vtc-XES spectra.

3. Results and discussions

3.1 Limitation of the XANES

Under reducing conditions, the Cu K-edge XANES of Cu-SSZ-13 samples have a feature peak around 8983 eV.[6, 7, 13, 14, 20, 36-39] This strong peak is recognized as a fingerprint of a Cu^+ cation with a linear configuration (unpublished results). Recent experimental results assigned this linear configuration to either O_{fw}-Cu^+-NH_3 or H_3N-Cu^+-NH_3 configurations in the NH_3_1_ZCu and NH_3_2_ZCu conformations respectively,[6, 7, 13, 14] where O_{fw} is a framework O atom of the zeolite. Our calculations also show that 1 or 2 NH_3 adsorbed on Cu^+ cations in ZCu or HZ_2Cu have linear configurations with either a O_{fw}-Cu^+-NH_3 or H_3N-Cu^+-NH_3 configuration, both of which are shown in Figure S1 of the Supporting Information. However, upon examination of the Cu K-edge XANES for these NH_3_1_ZCu and NH_3_2_ZCu conformations as shown in Figure 2b, the O_{fw}-Cu^+-NH_3 and H_3N-Cu^+-NH_3 sites are completely indistinguishable. Both could contribute to the peak around 8983 eV in the experimental XANES of a Cu-SSZ-13 sample under reducing conditions (1000 ppm NO, 1000 ppm NH_3 at 200 °C). Lamberti and coworkers also pointed out that the discrimination between the O_{fw}-Cu^+-NH_3 and the H_3N-Cu^+-NH_3 conformations remains an ongoing challenge because of their similar bond distances and angles.[14] Matthias Bauer commented that it is not possible to distinguish light atom ligands, such as carbon, nitrogen and oxygen atoms, in the proximity of the metal center.[11] As such, it is not possible to identify the ligand through a XANES analysis. We remark here that a well-defined second-shell peak characteristic of framework-coordinated species (such as O_{fw}-Cu^+-NH_3) was reported in an analysis of the EXAFS while it is absent in solution-like species such as H_3N-Cu^+-NH_3.[6, 13, 37] As discussed in the introduction, this may alternatively be overcome by employing vtc-XES.

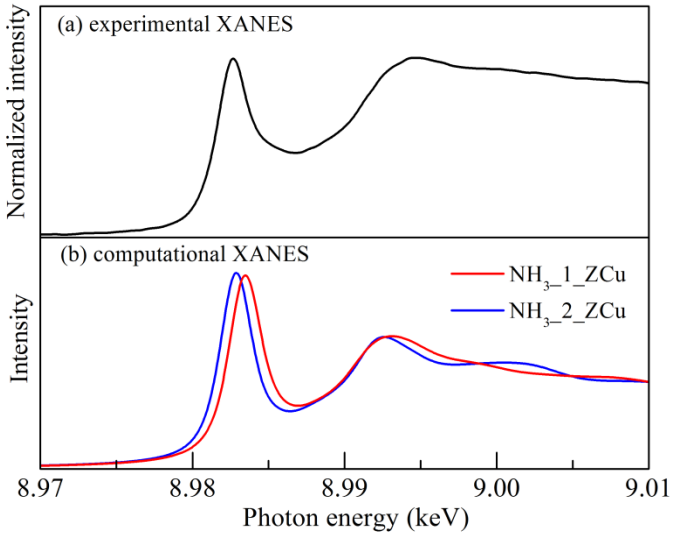

Figure 2. (a) Experimental Cu K-edge XANES for Cu-SSZ-13 sample (Cu/Al=0.02, Si/Al=4.5) under reducing conditions of 1000 ppm NO, 1000 ppm NH_3 at 200 °C. (b) Computational Cu K-edge XANES for the NH_3_1_ZCu and the NH_3_2_ZCu conformations.

3.2 Ligand identification of vtc-XES for O in H_2O and N in NH_3

Three types of O species will be examined in this work, namely, framework O (O_{fw}), O in OH species(O_{OH}) and O in H_2O (for simplicity, O represents an oxygen atom in H_2O). Figure 3 displays the XES comparison for O_{fw} with O and O_{OH} with O ligands in Cu-SSZ-13 conformations. The structures of Z_2Cu and H_2O_4_Z_2Cu are chosen to compare the sensitivity of Cu when bonded to either O_{fw} or O within a Z_2Cu or a H_2O_4_Z_2Cu conformation, which have 4 O_{fw} and 4 O ligands, respectively. As shown in Figure 3a, we find that the O ligand results in significant kβ″ and $k\beta_{2,5}$ shifts in the XES as compared to the O_{fw} ligands. The shifts are 1.7 and 1.8 eV for of kβ″ and $k\beta_{2,5}$ peaks, respectively. When comparing the O_{OH} and O ligands, as shown in Figure 3b, the difference between the Cu cations in the H_2O_4_Z_2Cu and H_2O_4_ZCuOH conformations consists of 1 O and 1 O_{OH} ligand (4 O vs 3 O and 1 O_{OH}). It turns out that the additional O ligand also has shifts of 1.3 and 0.8 eV for the kβ″ and the $k\beta_{2,5}$ XES peaks respectively as compared to the results of the structure with the O_{OH} ligand. As such, the three types of O(O_{fw}, O_{OH} and O) affect the location of the kβ″ and $k\beta_{2,5}$ emission lines. However, here we focus on the identification of O in H_2O and N in NH_3 in this work. Therefore, in the following results, we will not further examine the effect of O_{fw} and O_{OH} on the XES when comparing our XES results with either O or N bound Cu ligands.

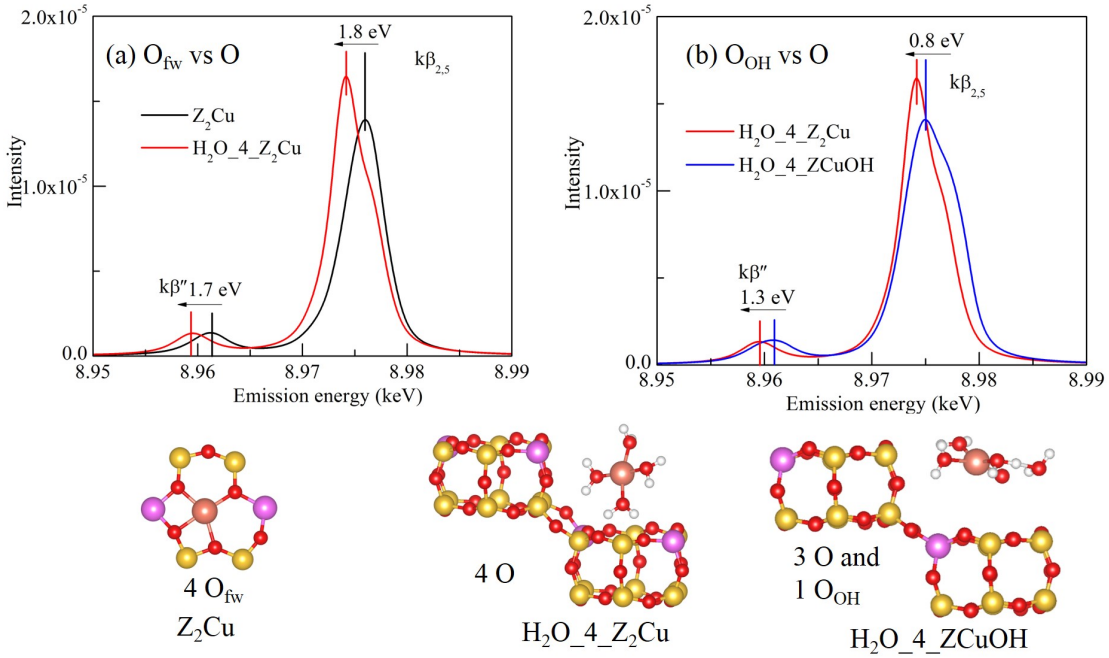

Figure 3. XES comparison for different types of O ligands, (a) O_{fw} vs O and (b)O_{OH} vs O. The structures of Z_2Cu, $H_2O\_4\_Z_2Cu$ and $H_2O\_4\_ZCuOH$ are shown in the bottom.

In order to further identify the ligand environments through vtc-XES, two structural models, $H_2O\_1\_ZCu$ and $NH_3\_1\_ZCu$, were chosen for further analysis. They both have a Cu^+ cation with a linear configuration, as shown in the insert of Figure 4. The only difference between these two structures is the Cu-O and Cu-N bond, where the O and N atoms are from an adsorbed H_2O and NH_3 molecule, respectively. Their corresponding vtc-XES results are shown in Figure 4. The two emission lines in the vtc-XES, noted as kβ″ and $kβ_{2,5}$, are related to the nature of the ligands coordinated to the metal centers.[11, 12, 18] This is clearly shown in the differences of the vtc-XES plots for the $H_2O\_1\_ZCu$ and $NH_3\_1\_ZCu$ conformations. Firstly, one can see a blue shift of about 0.9 eV for the kβ" lines, where the kβ" emission energy of the Cu ion in $NH_3\_1\_ZCu$ is higher than that in $H_2O\_1\_ZCu$. Secondly, $NH_3\_1\_ZCu$ has a stronger $kβ_{2,5}$ intensity line than $H_2O\_1\_ZCu$. As a result, one can distinguish between the adsorption of H_2O or NH_3 by the different vtc-XES emission lines of Cu-O and Cu-N. It also supports previous reports regarding the ability of vtc-XES to identify different ligands that are bonded to the Cu cations.[13, 14] The same conclusion can be reached for another type of Cu^+ cation environment in the $H_2O\_1\_HZ_2Cu$ and $NH_3\_1\_HZ_2Cu$ 2Al site conformations as shown in Figure S2 of the Supporting Information. The energy shift of the kβ" line between $H_2O\_1\_HZ_2Cu$ and $NH_3\_1\_HZ_2Cu$ is 1.5 eV, which is larger than that between $H_2O\_1\_ZCu$ and $NH_3\_1\_ZCu$. This implies that the presence of a Bronsted acid site could enhance the kβ" line shift energy between Cu-O and Cu-N ligation.

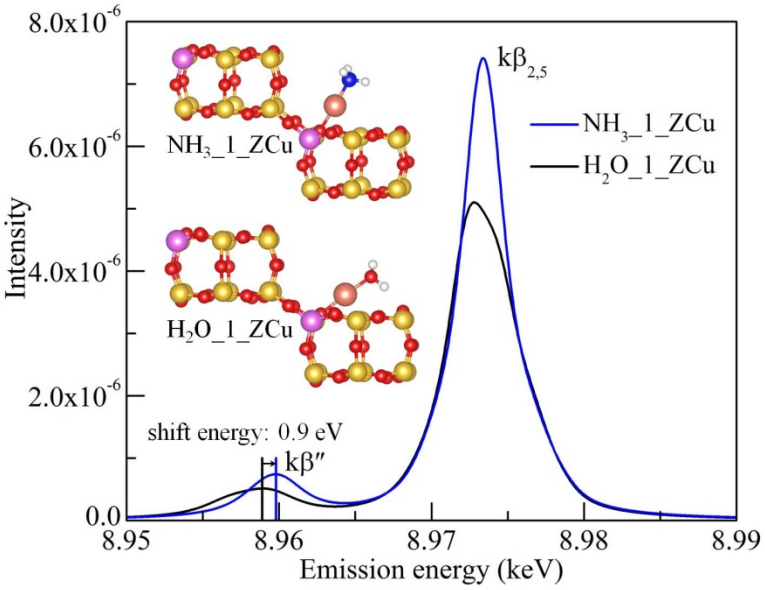

Figure 4. Computational vtc-XES of Cu ions in the H_2O_1_ZCu and NH_3_1_ZCu conformations. Two emission lines, kβ" and $k\beta_{2,5}$, are presented. The insert displays structures of the H_2O_1_ZCu and NH_3_1_ZCu conformations.

Moving forward to the Cu^{2+} cations in Cu-SSZ-13, the H_2O_1_Z_2Cu and NH_3_1_Z_2Cu conformations with of 2 Al sites were taken into consideration. Their structures are displayed as an insert to Figure 5. Cu^{2+} cations in H_2O_1_Z_2Cu and NH_3_1_Z_2Cu conformations have a coordination number of 4, which includes three framework O atoms and one O or N atom from adsorbed molecules. The only structural difference between H_2O_1_Z_2Cu and NH_3_1_Z_2Cu is the Cu-O or Cu-N bond. Similar with the difference of vtc-XES plots among H_2O_1_ZCu and NH_3_1_ZCu (shown in Figure 4), Cu^{2+} cations in H_2O_1_Z_2Cu and NH_3_1_Z_2Cu have a blue shift of about 0.9 eV for the kβ" lines and a stronger $k\beta_{2,5}$ intensity for the NH_3_1_Z_2Cu as presented in Figure 5. This result again confirms the ability of ligand identification for Cu cations through use of vtc-XES. However, for Cu^{2+} cations in the H_2O_1_ZCuOH and NH_3_1_ZCuOH conformations with one Al in the chabazite framework, the energy difference of the kβ" lines is very small (0.1 eV), which is shown in Figure S3 of the Supporting Information. This suggests that the formation of $[Cu^{2+}(OH^-)]^+$ species weakens the difference between the Cu-O and Cu-N ligation.

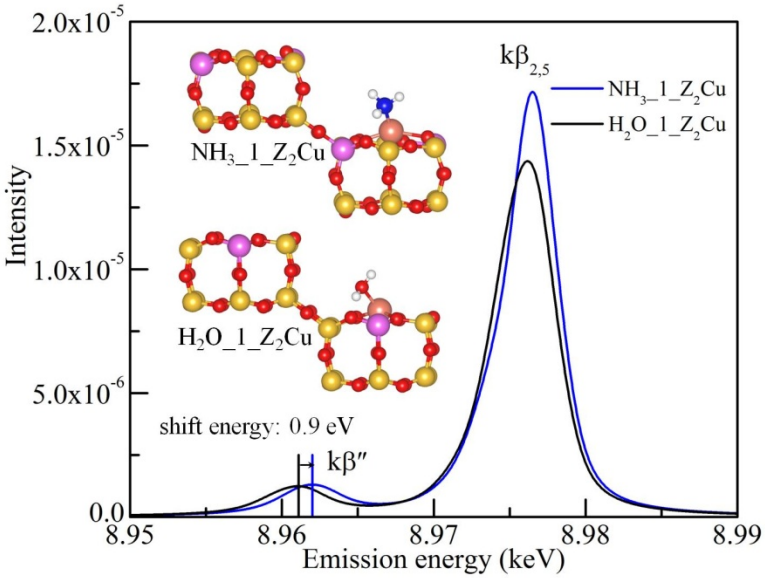

Figure 5. Computational vtc-XES of Cu cations in H_2O_1_Z_2Cu and NH_3_1_Z_2Cu. Two emission lines, kβ" and $k\beta_{2,5}$, are presented. The insert displays the H_2O_1_Z_2Cu and NH_3_1_Z_2Cu structures.

Overall, for both Cu^+ and Cu^{2+} cations in the Cu-SSZ-13 structure, the discrimination of the ligands containing O and N atoms can be revealed from the kβ″ and $k\beta_{2,5}$ lines in vtc-XES spectra. Note that in the above structures, the kβ″ shift energy between H_2O and NH_3 adsorbed Cu-SSZ-13 is only considered when a single Cu-O or Cu-N bond is varied. As such, a natural question that arises is whether the number of Cu-O or Cu-N bonds affects the energy shift of the kβ″ line in the corresponding emission spectra. To address this concern, we constructed structures with the same population of Cu-O and Cu-N bonds to model multiple H_2O and NH_3 adsorption on Cu-SSZ-13. Note that the population of Cu-O or Cu-N bonds doesn't include the contribution from framework oxygen atoms (population number ≠ coordination number). The population numbers for all structures studied in this work are shown in Figure S1 of the Supporting Information. For a Cu^+ cation, using ZCu for an example, H_2O_1_ZCu and NH_3_1_ZCu have a single Cu-O or Cu-N bond ($N_{population}$ = 1), respectively, while the H_2O_6_ZCu and NH_3_2_ZCu conformations have $N_{population}$ = 2 and the H_2O_4_ZCu and NH_3_3_ZCu conformations have $N_{population}$ = 3 (note that not all molecules absorb to the Cu ion). For Cu^{2+} cations, now using Z_2Cu as an example, the H_2O_1_Z_2Cu and NH_3_1_Z_2Cu conformations have $N_{population}$ = 1, while the H_2O_2_Z_2Cu and NH_3_2_Z_2Cu conformations have $N_{population}$ = 2 and the H_2O_4_Z_2Cu and NH_3_4_Z_2Cu conformations have $N_{population}$ = 4. These structures can be found in Figure S1 of the Supporting Information. The kβ″ line energy shift between the H_2O and NH_3 adsorbed species as a function of $N_{population}$ is shown in Figure 6. We find that the energy shift of the kβ″ line between H_2O and NH_3 adsorbed Cu-SSZ-13 increases with increasing $N_{population}$ for both the Cu^+ and Cu^{2+}

cations. Similar trends are also found for HZ_2Cu and ZCuOH conformations, which are shown in Figure S4 of the Supporting Information. As for the the energy shift trend of the kβ″ line, we also consider the relative fraction of $N_{population}$ of N and O with respect to the total number of bonds in the first coordination sphere of the Cu cation (i.e., the Cu cation coordination number), as shown in Figure 6.

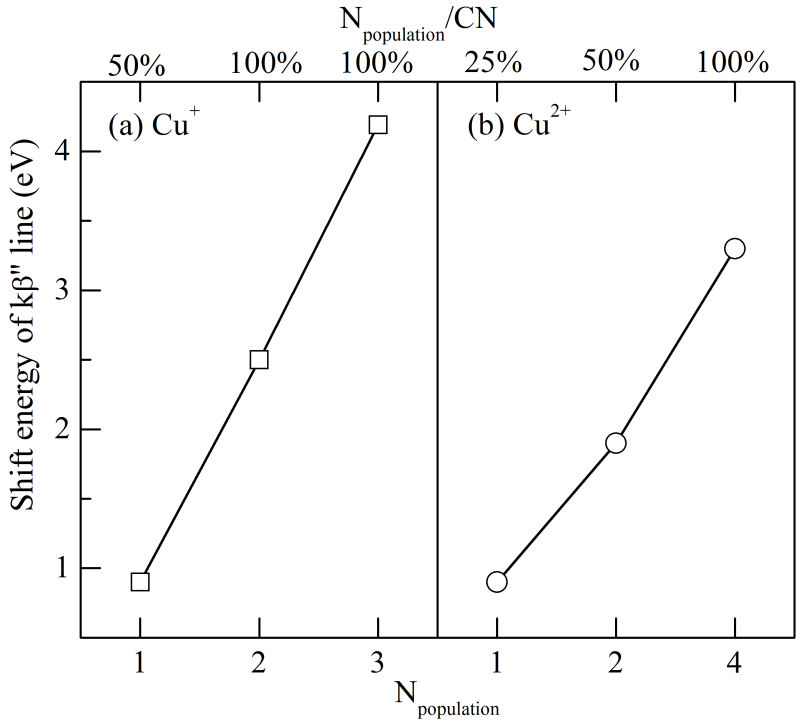

Figure 6. The energy shift of the kβ″ line between H_2O and NH_3 adsorbed Cu-SSZ-13 as a function of $N_{population}$ of H_2O and NH_3 for (a) a Cu^+ cation in ZCu and (b) a Cu^{2+} cation in Z_2Cu. The corresponding relative fractions of $N_{population}$ with respect to the total coordination number (CN) of Cu cations are shown in the top of the figure as $N_{population}/CN$.

3.3 Characterization of vtc-XES by varying the Cu oxidation state

Based on the results from the previous section, it is clear that vtc-XES has the ability to identify different ligand environments. In the discussion up to now, we fixed the oxidation state of Cu as either Cu^+ or Cu^{2+} and computed the XES while varying the ligand environment. As is well known from the XANES literature, one expects a higher edge position due to the higher binding energy of electrons when the exchanged cation is in a higher oxidation state. However, we recently have shown that this relationship is more complex (unpublished results). On the other hand, it is also important to understand the relationship between the emission lines energies in vtc-XES and the oxidation state of the metal exchanged ion. Figure 7 shows the simulated kβ″

and $k\beta_{2,5}$ peaks of vtc-XES spectra of Cu cations that have the same ligand environment when its oxidation state is varied. We find that both the location of $k\beta''$ and $k\beta_{2,5}$ lines shift slightly as the oxidation state of Cu shifts from Cu^{+} to Cu^{2+}, although the intensity of the $k\beta''$ and the $k\beta_{2,5}$ lines changes significantly. This result is consistent with the experimental results reported by Borfecchia *et al.*,[21] where He-activated and O_2-actived samples (represent Cu^{+} and Cu^{2+}, respectively) have same location of the $k\beta''$ line.

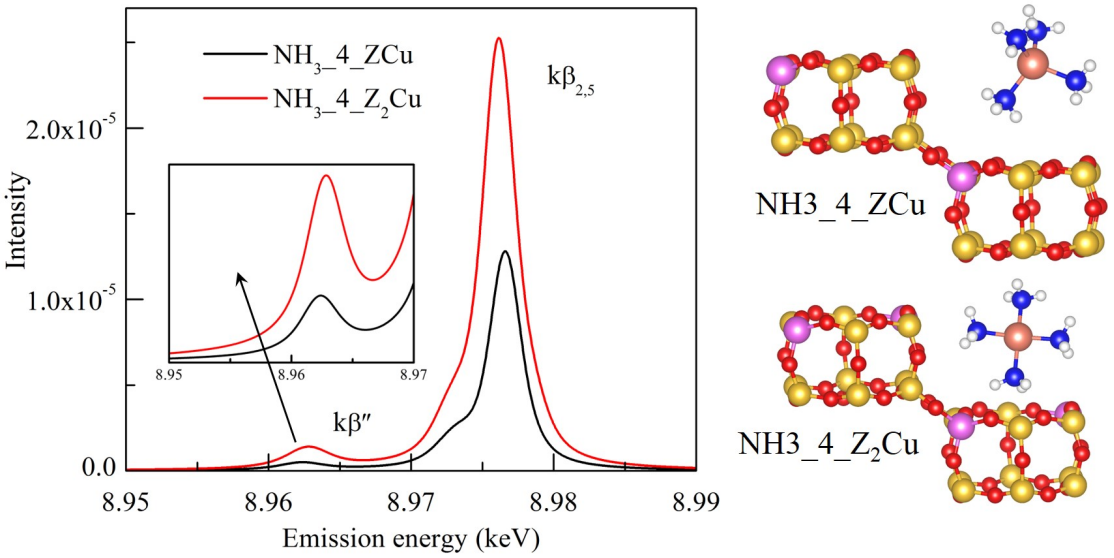

Figure 7. Comparison of vtc-XES of Cu^{+} and Cu^{2+} cations in same ligand environment (4 NH_3) with a NH_3_4_ZCu and a NH_3_4_Z_2Cu conformation, respectively.

3.4 PDOS analysis and chemical sensitivity of the ligand for vtc-XES

To investigate in detail the origins of the valence-to-core $k\beta''$ and $k\beta_{2,5}$ lines, PDOS and orbital calculations are employed using the final state wavefunction where a core hole is created in the exchanged Cu cation. For simplicity, the NH_3_2_ZCu structure was analyzed due to its linear, symmetric N-Cu-N configuration as shown in Figure S1 of the Supporting Information. The calculated Cu vtc-XES and corresponding PDOS for the Cu and N atoms are presented in Figure 8. We find that the emission energy of the kβ" line correlates very well with the N 2*s* peak position around 8960 eV. The orbital distribution also clearly shows that the N 2*s* orbitals mainly contribute to the kβ" emission line at 8960 eV. This shows that the kβ" emission line arises from a transition from the N 2*s* electron to the Cu 1*s* core hole. This statement not only applies to Cu[14] but also to other metal centers.[16] In other words, the emission energy of the $k\beta''$ line is determined by the binding energy of ligand 2*s* orbital.

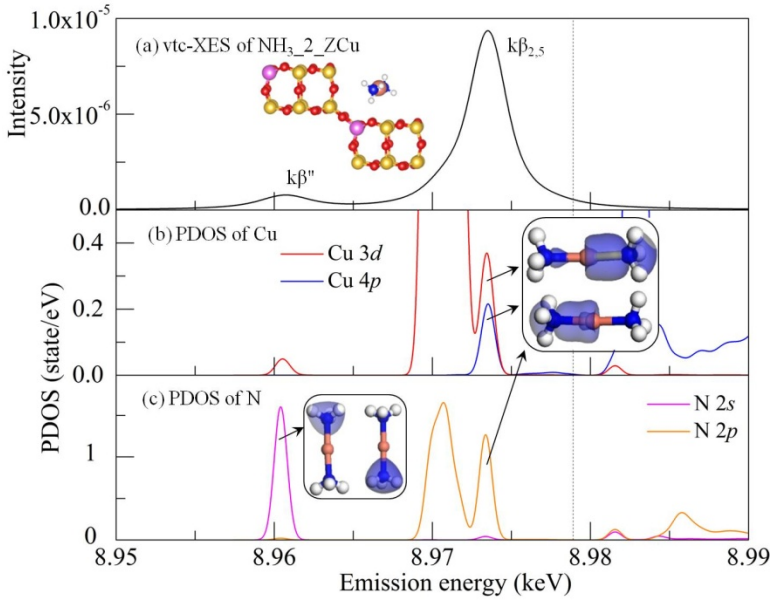

Figure 8. The calculated (a) vtc-XES of NH_3_2_ZCu, PDOS of (b) Cu and (c) N. The vertical dashed line at 8978.9 eV shows the Fermi level. The NH_3_2_ZCu structure, orbital distribution in the 8960 and 8973 eV energy range are displayed as inserts in (a), (b) and (c), respectively. The iso-surface value of the orbital distribution is 0.04 electrons/Å^3.

For the k$\beta_{2,5}$ emission line, we find that the emission energy correlates well to a mixture of N 2*p*, Cu 3*d* and 4*p* states in the 8973 eV energy range. Compared to the 8971 eV energy range where vtc-XES doesn't have an emission line but has a large Cu 3d character, the 8973 eV energy range is mainly due to contributions from the Cu 4*p* state. This means that the Cu 4*p* state plays a key role in generating the k$\beta_{2,5}$ emission line. However, for Cu cations, the Cu 4*p* state is supposed to be distributed above the Fermi level. We can rationalize that the appearance of Cu 4*p* state below the Fermi level originates from an orbital mixing with the Cu 3*d* state.[16] As displayed in Figure 8b, the orbital distribution also clearly shows that the Cu and N atoms both contribute to the states around 8973 eV. Therefore, we conclude that the k$\beta_{2,5}$ emission line is generated from the transition that mixes the N 2*p*, Cu 3*d* and 4*p* states to the Cu 1*s* core hole, where the Cu 4*p* state plays a key role in this transition.

Based on the above analysis, it is clear that the kβ" emission line is generated by a ligand 2*s* to Cu 1*s* transition. To understand the chemical sensitivity of vtc-XES on the bonding of the Cu ligand, we plot the PDOS of the N 2s and O 2s for the H_2O_1_ZCu and NH_3_1_ZCu in Figure 9. In order to interpret the ability of vtc-XES to identify the ligand environment (shown in Figure 3), we compare the PDOS of O 2*s* state of H_2O_1_ZCu and that of N 2*s* state of NH_3_1_ZCu, as shown in Figure 9. We find that the N 2*s* state has a higher binding energy than the O 2*s* state. This result lies at the origin of the ligand identification using vtc-XES in which different ligands

have different 2s state binding energies. It is clear that the chemical sensitivity of the vtc-XES is due to the ligand environment and is intrinsically determined by the different binding energies of the ligand 2s state. Note that the interpretation of $k\beta_{2,5}$ emission line is more complex than that of the kβ" emission line. Further studies are needed to understand the $k\beta_{2,5}$ emission line at an electronic level.

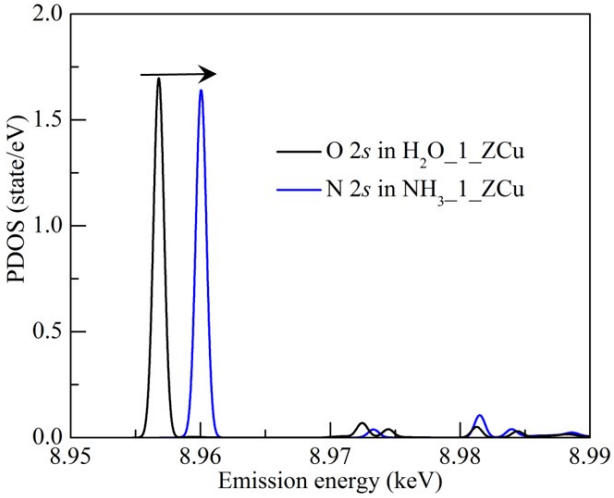

Figure 9. PDOS analysis of the O 2*s* in H_2O_1_ZCu, as well as the N 2*s* and in NH_3_1_ZCu, so as to interpret the bonding ligand effect on the emission spectra.

3.5 Feedback to experimental results

We compared our computational vtc-XES results with the experimental data that is available in the literature[13]. As shown in Figure 10a, the red, gray and red vtc-XES spectra are assigned to the ZCuOH, H_2O_6_Z_2Cu and NH_3_2_ZCu structures[13]. The corresponding computational vtc-XES spectra are shown in Figure 10b. We find that the computational vtc-XES spectra for ZCuOH and H_2O_6_Z_2Cu are in good agreement with the experimental ones. However, the computational vtc-XES results of NH_3_2_ZCu shows totally different emission lines, including the intensity and locations with respect to that of ZCuOH and H_2O_6_Z_2Cu conformations. The assignment of NH_3_2_ZCu was made by concluding that a Cu^{2+} cation in a Cu-SSZ-13 sample could be reduced to Cu^+ in presence of NO and NH_3.[7,13,37] We reconsider this assignment and propose that Cu^{2+} ion probably was not completely reduced to Cu^+ ion when exposed to NO and NH_3, where the $[Cu(NH_3)_4]^{2+}$ could be formed. In Figure 10c, the computational vtc-XES spectra of ZCuOH, H_2O_6_Z_2Cu and NH_3_4_Z_2Cu conformations are plotted, which are consistent with the experimental results in Figure 10a. This suggests that the reduction of Cu^{2+} when exposed to NO and NH_3 is perhaps more complex than originally suggested in literature.

The assignment of a Cu^+ cation was originally made in the literature because of the large peak around 8984 eV that was observed experimentally in the XANES when Cu-SSZ-13 is

exposed to NO and NH_3.[7, 13] Additionally, it was also reported that the exposure of oxidized Cu-SSZ-13 to NO+NH_3 at 200 °C results in a Cu^+ species since a drastic abatement of the EPR signal was observed.[38] Further evidence of a Cu^+ species arises from the absence of a pre-edge peak deriving from a 1s to 3d transition,[6,13,38] and by comparing the similar XANES and EXAFS features when Cu-SSZ-13 is exposed to NO+NH_3 to those of a reference $[Cu(NH_3)_2]^+$ compound in the solution phase.[13,38,39] However, the comparison between the computational and experimental XES suggests a different assignment on Cu-SSZ-13 when exposed to NO and NH_3, as shown in Figure 10a-c. As such, a natural question that arises is whether the XANES spectrum of a Cu^+ cation bonded to two NH_3 and a Cu^{2+} cation bonded to four NH_3 have peaks that are located in the same photon energy range. In Figure 10d, we compare the XANES spectra of these two conformations. Figure 10d shows that $[Cu(NH_3)_2]^+$ has a peak with a strong intensity around 8984 eV, while $[Cu(NH_3)_4]^{2+}$ has a peak with a weak intensity in the same photon energy range. As such, both species could contribute to the peak around 8984 eV in the experimental XANES when Cu-SSZ-13 is exposed to NO+NH_3.

Finally, it is also interesting to note that the intensity of the 8984 eV peak is much greater than of the 8994 eV peak in the NH_3_2_ZCu conformation, which is not in agreement with the experimental observations where, depending on the reaction conditions, the intensity of the 8984 eV peak is found to be similar or smaller to that of the 8994 eV peak.[7, 13] We also note, as discussed in our previous work,[4] that the computed XANES in Figure 10d also differs to that of the experimental $[Cu(NH_3)_4]^{2+}$ reference compound when put in an aqueous solution, since the presence of water significantly affects the computed XANES spectrum by shifting the photon energy of the white to higher computed values as well as affecting its peak shape. As such, we do not expect the XANES spectra as shown in Figure 10d to be identical to what was found in the literature for the experimental $[Cu(NH_3)_2]^+$ and $[Cu(NH_3)_4]^{2+}$ reference compounds,[38] which will both surely interact with water when put in an aqueous solution. In sum, these results suggest an open question that would need to be revisited with regard to the interpretation of the XANES features, for which the appearance of a $[Cu(NH_3)_2]^+$ species in the corresponding SCR reaction mechanism has been proposed in the literature for Cu-SSZ-13.[15,37]

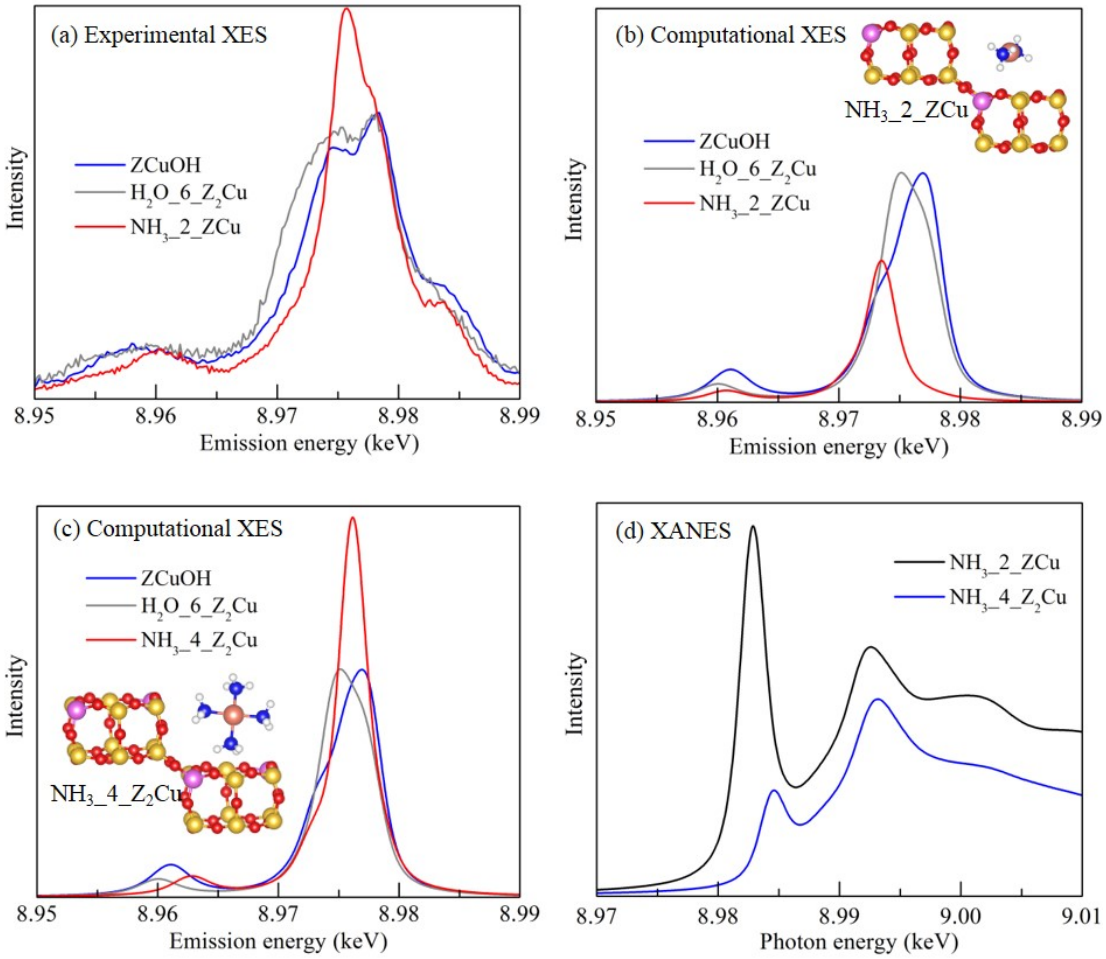

Figure 10. (a) Plot of experimental vtc-XES data for ZCuOH (blue solid line), $H_2O\_6\_Z_2Cu$ gray solid line and $NH_3\_2\_ZCu$ (red solid line) from reference[13]. Computational XES for (b) the ZCuOH, $H_2O\_6\_Z_2Cu$ and $NH_3\_2\_ZCu$ conformations, (c) the ZCuOH, $H_2O\_6\_Z_2Cu$ and $NH_3\_4\_Z_2Cu$ conformations. The structures of $NH_3\_2\_ZCu$ and $NH_3\_4\_Z_2Cu$ are displayed in (b) and (c) respectively. (d) Computational XANES for $NH_3\_2\_ZCu$ and $NH_3\_4\_Z_2Cu$ conformations.

4. Conclusions

In this study, the chemical sensitivity of vtc-XES due to the ligand environment and the oxidation state of the metal exchanged ion was investigated using DFT calculations. It is found that the vtc-XES can overcome the ligand identification limitation of XANES. By comparing vtc-XES of $H_2O\_1\_ZCu$ and $NH_3\_1\_ZCu$ conformations, we found the kβ" lines shifted by about 0.9 eV, meaning that the kβ" emission energy of a Cu cation in $NH_3\_1\_ZCu$ is higher than that in $H_2O\_1\_ZCu$. In addition, $NH_3\_1\_ZCu$ has a $k\beta_{2,5}$ line of stronger intensity than that of $H_2O\_1\_ZCu$ conformation. Therefore, one can discriminate the adsorption of H_2O or NH_3 due to the different vtc-XES emission lines resulting from Cu-O and Cu-N bonds. In addition, the presence of a Bronsted acid site could enhance the kβ" line shift energy between Cu-O and Cu-N

ligation for a Cu^{+} cation. Similar conclusions are also obtained for Cu^{2+} cations and the formation of $[Cu^{2+}(OH^{-})]^{+}$ species, which weakens the difference between Cu-O and Cu-N ligation. When examining the vtc-XES of multiple H_2O and NH_3 adsorbed Cu-SSZ-13 structures, it is found that the shifts of the kβ″ energy line between H_2O and NH_3 adsorbed Cu-SSZ-13 increases when increasing the population of Cu-ligand bonds for both Cu^{+} and Cu^{2+} cations. The effect of oxidation state on vtc-XES was also studied. We concluded that the variation of oxidation state slightly changes the emission lines peak positions while the corresponding intensity changes significantly. By performing a PDOS analysis, the kβ" emission line is generated by N 2*s* to Cu 1*s* transition while the $k\beta_{2,5}$ emission line is generated from a transition mixing the N 2*p*, Cu 3*d* and 4*p* states to the Cu 1*s* core hole, where the Cu 4*p* state plays key role in this transition.

Supporting Information

Optimized structures of multiple NH_3 and H_2O (n=1 to 6) adsorbed on Cu-SSZ-13 (ZCu, HZ_2Cu, Z_2Cu and ZCuOH). Computational vtc-XES of Cu ions in HZ_2Cu and ZCuOH. The shift energy of the kβ″ line as a function of $N_{population}$ for a Cu^{+} cation in HZ_2Cu and a Cu^{2+} cation in ZCuOH.

Acknowledgements

This work was supported by the National Science Foundation GOALI program under contract No. CBET-1258717. A portion of the computer time for the computational work was performed using EMSL, a national scientific user facility sponsored by the Department of Energy′s office of Biological and Environmental Research and located at PNNL. PNNL is a multi-program national laboratory operated for the US DOE by Battelle. HL acknowledges the financial supports of the National Natural Science Foundation of China (grant No. 11404235), and also supported by Program for the Top Young Academic Leaders of Higher Learning Institutions of Shanxi. We thank Mr. Kyle Groden, Dr. Janos Szanyi and Dr. Feng Gao for their useful suggestions and comments. We also thank Prof. Fabio Ribeiro for the experimental XANES data and Prof. Borfecchia for the experimental XES results.

References

1. Kwak, J. H.; Tonkyn, R. G.; Kim, D. H.; Szanyi, J.; Peden, C. H. F., Excellent Activity and Selectivity of Cu-SSZ-13 in the Selective Catalytic Reduction of NOx with NH3. *J. Catal.* **2010,** *275*, 187-190.

2. Kwak, J. H.; Tran, D.; Burton, S. D.; Szanyi, J.; Lee, J. H.; Peden, C. H. F., Effects of Hydrothermal Aging on NH3-SCR Reaction over Cu/zeolites. *J. Catal.* **2012,** *287*, 203-209.

3. Zhang, R.; McEwen, J.-S.; Kollár, M.; Gao, F.; Wang, Y.; Szanyi, J.; Peden, C. H. F., NO Chemisorption on Cu/SSZ-13: A Comparative Study from Infrared Spectroscopy and DFT Calculations. *ACS Catal.* **2014,** *4*, 4093-4105.

4. Zhang, R.; Szanyi, J.; Gao, F.; McEwen, J.-S., The Interaction of Reactants, Intermediates

and Products with Cu Ions in Cu-SSZ-13 NH_3 SCR Catalysts: An Energetic and Ab initio X-ray Absorption Modeling Study. *Catal. Sci. Tech.* **2016,** *6*, 5812-5829.

5. Zhang, R.; Helling, K.; McEwen, J.-S., Ab initio X-ray Absorption Modeling of Cu-SAPO-34: Characterization of Cu Exchange Sites under Different Conditions. *Catal. Today* **2016,** *267*, 28-40.

6. Paolucci, C.; Parekh, A. A.; Khurana, I.; Di Iorio, J. R.; Li, H.; Albarracin Caballero, J. D.; Shih, A. J.; Anggara, T.; Delgass, W. N.; Miller, J. T. et al, Catalysis in a Cage: Condition-Dependent Speciation and Dynamics of Exchanged Cu Cations in SSZ-13 Zeolites. *J. Am. Chem. Soc.* **2016,** *138*, 6028-6048.

7. Paolucci, C.; Verma, A. A.; Bates, S. A.; Kispersky, V. F.; Miller, J. T.; Gounder, R.; Delgass, W. N.; Ribeiro, F. H.; Schneider, W. F., Isolation of the Copper Redox Steps in the Standard Selective Catalytic Reduction on Cu-SSZ-13. *Angew. Chem. Int. Ed.* **2014,** *53*, 11828-11833.

8. Timoshenko, J.; Shivhare, A.; Scott, R. W. J.; Lu, D.; Frenkel, A. I., Solving Local Structure around Dopants in Metal Nanoparticles with Ab initio Modeling of X-ray Absorption Near Edge Structure. *Phys. Chem. Chem. Phys.* **2016,** *18*, 19621-19630.

9. McEwen, J. S.; Anggara, T.; Schneider, W. F.; Kispersky, V. F.; Miller, J. T.; Delgass, W. N.; Ribeiro, F. H., Integrated Operando X-ray Absorption and DFT Characterization of Cu–SSZ-13 Exchange Sites during the Selective Catalytic Reduction of NOx with NH3. *Catal. Today* **2012,** *184*, 129-144.

10. Lezcano-Gonzalez, I.; Wragg, D. S.; Slawinski, W. A.; Hemelsoet, K.; Van Yperen-De Deyne, A.; Waroquier, M.; Van Speybroeck, V.; Beale, A. M., Determination of the Nature of the Cu Coordination Complexes Formed in the Presence of NO and NH_3 within SSZ-13. *J. Phys. Chem. C* **2015,** *119*, 24393-24403.

11. Bauer, M., HERFD-XAS and Valence-to-core-XES: New Tools to Push the Limits in Research with Hard X-rays? *Phys. Chem. Chem. Phys.* **2014,** *16*, 13827-13837.

12. Gallo, E.; Glatzel, P., Valence to Core X-ray Emission Spectroscopy. *Adv. Mater.* **2014,** *26*, 7730-7746.

13. Lomachenko, K. A.; Borfecchia, E.; Negri, C.; Berlier, G.; Lamberti, C.; Beato, P.; Falsig, H.; Bordiga, S., The Cu-CHA deNOx Catalyst in Action: Temperature-Dependent NH_3-Assisted Selective Catalytic Reduction Monitored by Operando XAS and XES. *J. Am. Chem. Soc.* **2016,** *138*, 12025-12028.

14. Giordanino, F.; Borfecchia, E.; Lomachenko, K. A.; Lazzarini, A.; Agostini, G.; Gallo, E.; Soldatov, A. V.; Beato, P.; Bordiga, S.; Lamberti, C., Interaction of NH_3 with Cu-SSZ-13 Catalyst:

A Complementary FTIR, XANES, and XES Study. *J. Phys. Chem. Lett.* **2014,** *5*, 1552-1559.

15. Gao, F.; Mei, D.; Wang, Y.; Szanyi, J.; Peden, C. H. F., Selective Catalytic Reduction over Cu/SSZ-13: Linking Homo- and Heterogeneous Catalysis. *J. Am. Chem. Soc.* **2017,** *139*, 4935-4942.

16. Pollock, C. J.; DeBeer, S., Valence-to-Core X-ray Emission Spectroscopy: A Sensitive Probe of the Nature of a Bound Ligand. *J. Am. Chem. Soc.* **2011,** *133*, 5594-5601.

17. Vegelius, J. R.; Kvashnina, K. O.; Klintenberg, M.; Soroka, I. L.; Butorin, S. M., Cu $K\beta_{2,5}$ X-ray Emission Spectroscopy as a Tool for Characterization of Monovalent Copper Compounds. *J. Anal. At. Spectrom.* **2012,** *27*, 1882-1888.

18. Boubnov, A.; Carvalho, H. W. P.; Doronkin, D. E.; Günter, T.; Gallo, E.; Atkins, A. J.; Jacob, C. R.; Grunwaldt, J.-D., Selective Catalytic Reduction of NO Over Fe-ZSM-5: Mechanistic Insights by Operando HERFD-XANES and Valence-to-Core X-ray Emission Spectroscopy. *J. Am. Chem. Soc.* **2014,** *136*, 13006-13015.

19. Glatzel, P.; Bergmann, U., High Resolution 1s Core Hole X-ray Spectroscopy in 3d Transition Metal Complexes—Electronic and Structural Information. *Coord. Chem. Rev.* **2005,** *249*, 65-95

20. Gunter, T.; Carvalho, H. W. P.; Doronkin, D. E.; Sheppard, T.; Glatzel, P.; Atkins, A. J.; Rudolph, J.; Jacob, C. R.; Casapu, M.; Grunwaldt, J.-D., Structural Snapshots of the SCR Reaction Mechanism on Cu-SSZ-13. *Chem. Comm.* **2015,** *51*, 9227-9230.

21. Borfecchia, E.; Lomachenko, K. A.; Giordanino, F.; Falsig, H.; Beato, P.; Soldatov, A. V.; Bordiga, S.; Lamberti, C., Revisiting the Nature of Cu Sites in the Activated Cu-SSZ-13 Catalyst for SCR Reaction. *Chem. Sci.* **2015,** *6*, 548-563.

22. Kresse, G.; Furthmüller, J., Efficient Iterative Schemes for Ab initio Total-energy Calculations Using a Plane-wave Basis set. *Phys. Rev. B* **1996,** *54*, 11169.

23. Kresse, G.; Hafner, J., Ab initio Molecular Dynamics for Liquid Metals. *Phys. Rev. B* **1993,** *47*, 558.

24. Blöchl, P. E., Projector Augmented-wave Method. *Phys. Rev. B* **1994,** *50*, 17953.

25. Kresse, G.; Joubert, D., From Ultrasoft Pseudopotentials to the Projector Augmented-wave Method. *Phys. Rev. B* **1999,** *59*, 1758-1775.

26. Perdew, J. P.; Wang, Y., Accurate and Simple Analytic Representation of the Electron-gas Correlation Energy. *Phys. Rev. B* **1992,** *45*, 13244.

27. Itho, Y.; Nishiyama, S.; Tsuruya, S.; Masai, M., Redox Behavior and Mobility of Copper Ions in NaZSM-5 Zeolite during Oxidation. *J. Phys. Chem.* **1994,** *98*, 960-967.

28. Kispersky, V. F.; Kropf, A. J.; Ribeiro, F. H.; Miller, J. T., Low Absorption Vitreous

Carbon Reactors for Operando XAS: A Case Study on Cu/Zeolites for Selective Catalytic Reduction of NOx by NH3. *Phys. Chem. Chem. Phys.* **2012,** *14*, 2229-2238.

29. Gao, F.; Kwak, J.; Szanyi, J.; Peden, C. F., Current Understanding of Cu-Exchanged Chabazite Molecular Sieves for Use as Commercial Diesel Engine DeNOx Catalysts. *Top. Catal.* **2013,** *56*, 1441-1459.

30. Gao, F.; Walter, E. D.; Kollar, M.; Wang, Y.; Szanyi, J.; Peden, C. H. F., Understanding Ammonia Selective Catalytic Reduction Kinetics over Cu/SSZ-13 from Motion of the Cu Ions. *J. Catal.* **2014,** *319*, 1-14.

31. Giordanino, F.; Vennestrom, P. N. R.; Lundegaard, L. F.; Stappen, F. N.; Mossin, S.; Beato, P.; Bordiga, S.; Lamberti, C., Characterization of Cu-exchanged SSZ-13: A Comparative FTIR, UV-Vis, and EPR Study with Cu-ZSM-5 and Cu-β with Similar Si/Al and Cu/Al Ratios. *Dalton Trans.* **2013,** *42*, 12741-12761.

32. Lezcano-Gonzalez, I.; Deka, U.; Arstad, B.; Van Yperen-De Deyne, A.; Hemelsoet, K.; Waroquier, M.; Van Speybroeck, V.; Weckhuysen, B. M.; Beale, A. M., Determining the Storage, Availability and Reactivity of NH3 within Cu-Chabazite-based Ammonia Selective Catalytic Reduction Systems. *Phys. Chem. Chem. Phys.* **2014,** *16*, 1639-1650.

33. Clark, S. J.; Segall, M. D.; Pickard, C. J.; Hasnip, P. J.; Probert, M. J.; Refson, K.; Payne, M. C., First Principles Methods using CASTEP. *Z. Kristallogr.* **2005,** *220*, 567-570.

34. Gao, S.-P.; Pickard, C. J.; Perlov, A.; Milman, V., Core-level Spectroscopy Calculation and the Plane Wave Pseudopotential Method. *J. Phys. Condens. Matter* **2009,** *21*, 104203.

35. Mo, S.-D.; Ching, W. Y., X-ray Absorption Near-edge Structure in Alpha-quartz and Stishovite: Ab initio Calculation with Core–hole Interaction. *Appl. Phys. Lett.* **2001,** *78*, 3809-3811.

36. Bates, S. A.; Verma, A. A.; Paolucci, C.; Parekh, A. A.; Anggara, T.; Yezerets, A.; Schneider, W. F.; Miller, J. T.; Delgass, W. N.; Ribeiro, F. H., Identification of the Active Cu Site in Standard Selective Catalytic Reduction with Ammonia on Cu-SSZ-13. *J. Catal.* **2014,** *312*, 87-97.

37. Janssens, T. V. W.; Falsig, H.; Lundegaard, L. F.; Vennestrøm, P. N. R.; Rasmussen, S. B.; Moses, P. G.; Giordanino, F.; Borfecchia, E.; Lomachenko, K. A.; Lamberti, C. et al, A Consistent Reaction Scheme for the Selective Catalytic Reduction of Nitrogen Oxides with Ammonia. *ACS Catal.* **2015,** *5*, 2832-2845.

37. C. Paolucci, I. Khurana, A. A. Parekh, S. Li, A. J. Shih, H. Li, J. R. Di Iorio, J. D. Albarracin-Caballero, A. Yezerets, J. T. Miller, W. N. Delgass, F. H. Ribeiro, W. F. Schneider, R.

Gounder, Dynamic Multinuclear Sites Formed by Mobilized Copper Ions in NO_x Selective Catalytic Reduction, *Science* **2017**, 357, 898-903.

38. Lamble, G.; Moen, A.; Nicholson, D. G., Structure of the Diamminecopper(I) Ion in Solution. An X-ray Absorption Spectroscopic Study. *J. Chem. Soc. Faraday Trans.* **1994,** *90*, 2211-2213.

39. Kau, L. S.; Spira-Solomon, D. J.; Penner-Hahn, J. E.; Hodgson, K. O.; Solomon, E. I., X-ray Absorption Edge Determination of the Oxidation State and Coordination Number of Copper: Application to the Type 3 Site in *Rhus vernicifera* Laccase and Its Reaction with Oxygen. *J. Am. Chem. Soc.* **1987,** *109*, 6433-6442.

530 TOC Graphic

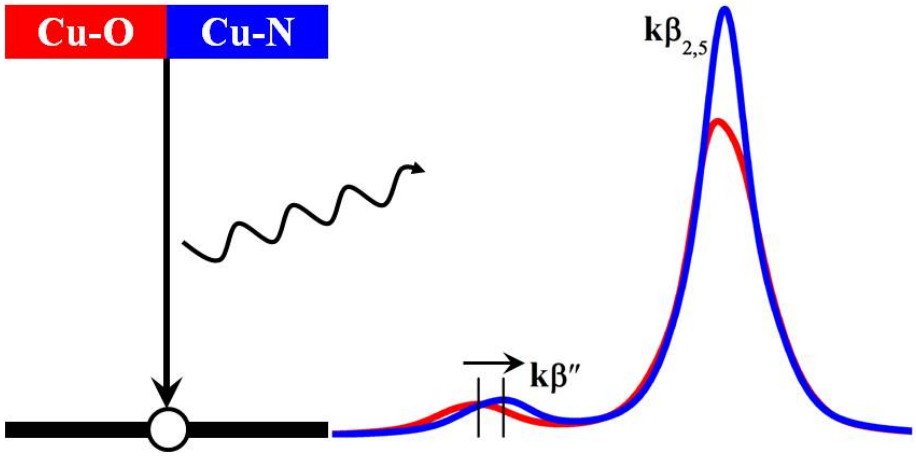

531

Supporting Information

Chemical sensitivity of Valence-to-core X-ray Emission Spectroscopy due to Ligand and Oxidation State: A Computational Study on Cu-SSZ-13 with Multiple H_2O and NH_3 Adsorption

Renqin Zhang[a]†, Hui Li[a,b]†, Jean-Sabin McEwen[a,c,d,e*]

[a]*The Gene and Linda Voiland School of Chemical Engineering and Bioengineering, Washington State University, Pullman, WA 99164*

[b]*College of Materials Science and Engineering, Taiyuan University of Technology, Taiyuan, China 030024*

[c]*Department of Physics and Astronomy, Washington State University, Pullman, WA 99164*

[d]*Department of Chemistry, Washington State University, Pullman, WA 99164*

[e]*Institute for Integrated Catalysis, Pacific Northwest National Laboratory, Richland, WA, 99352*

†Contribute equally; *Corresponding author: js.mcewen@wsu.edu

H_2O on ZCu

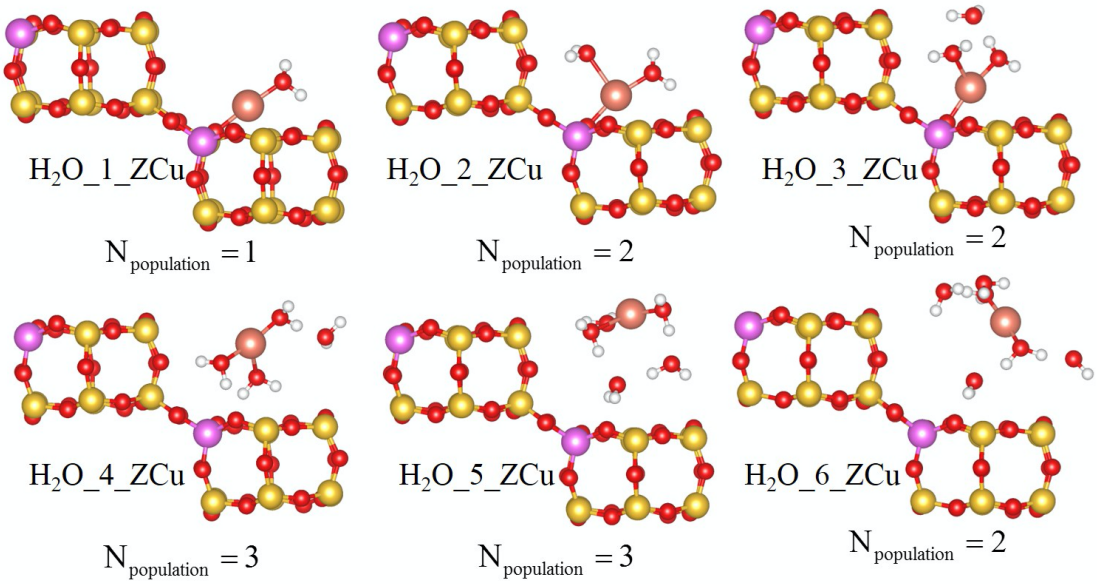

NH_3 on ZCu

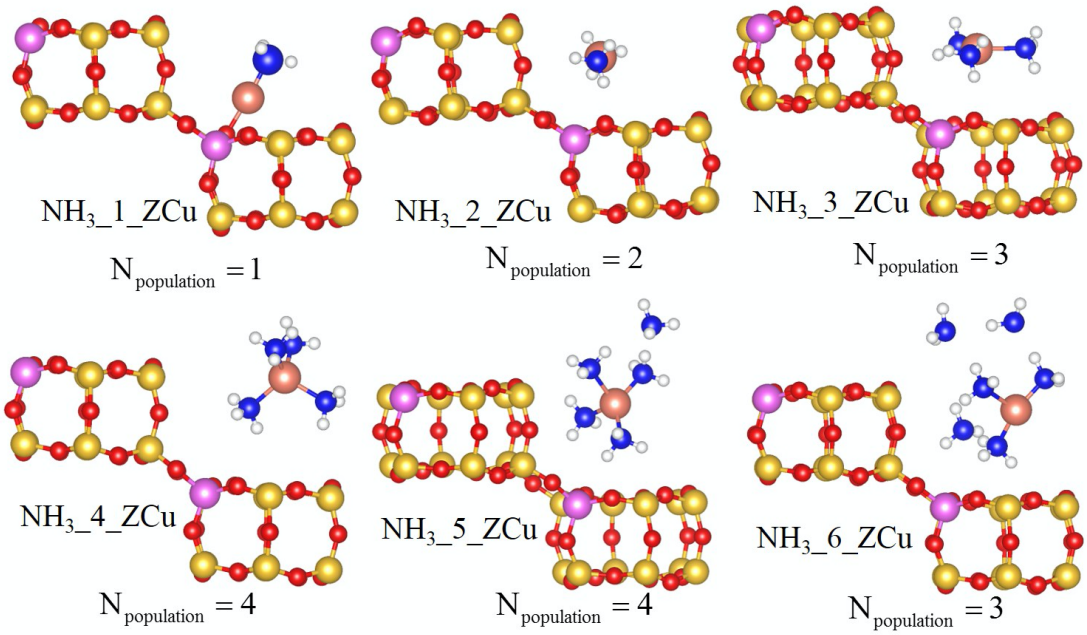

H_2O on HZ_2Cu

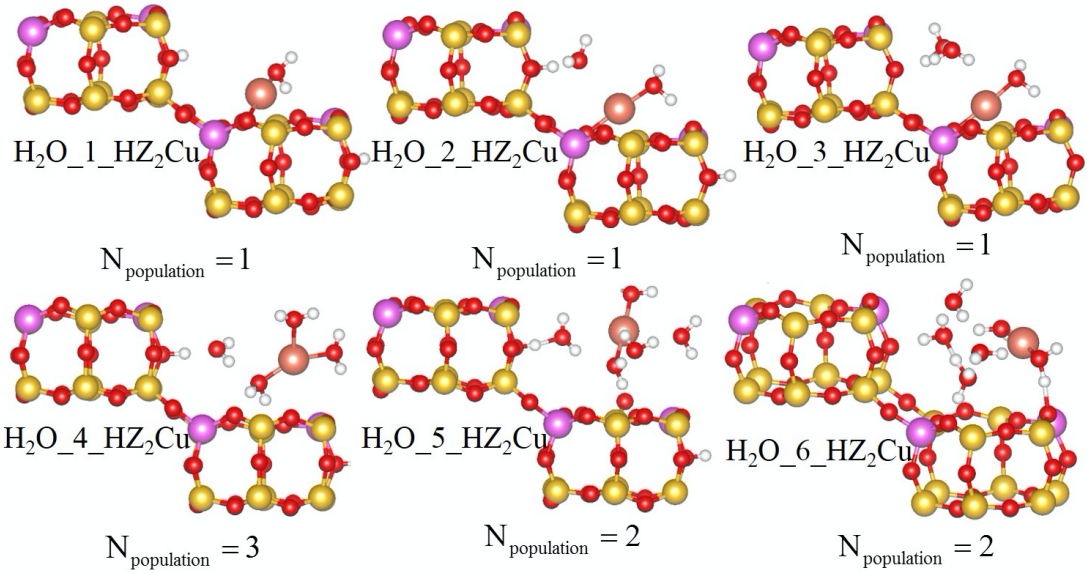

NH_3 on HZ_2Cu

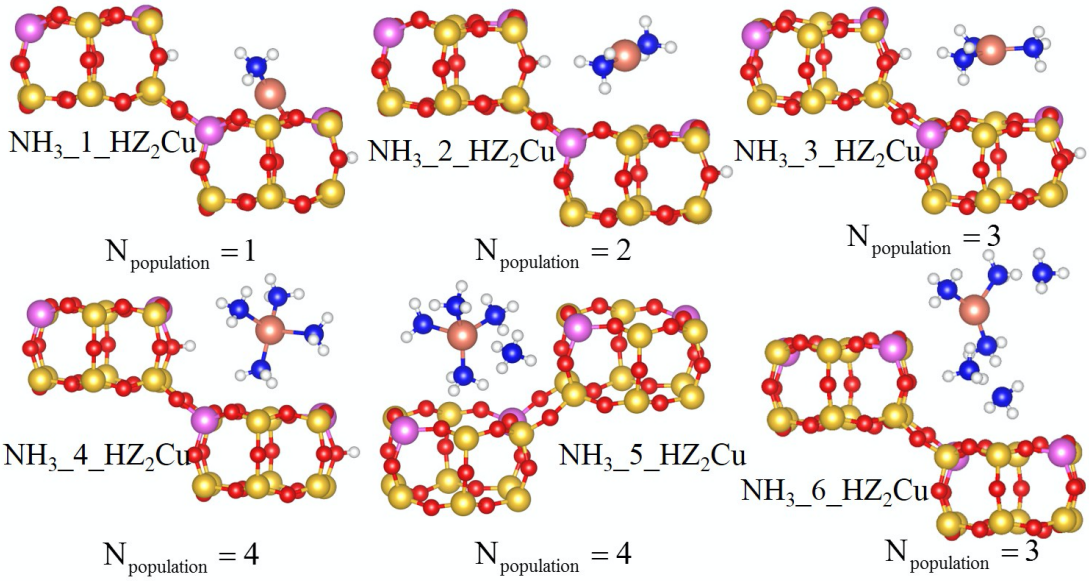

H_2O on Z_2Cu

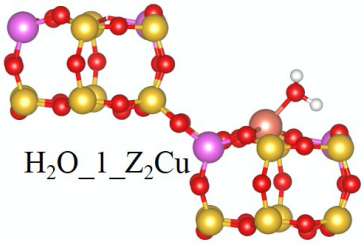

$N_{population} = 1$

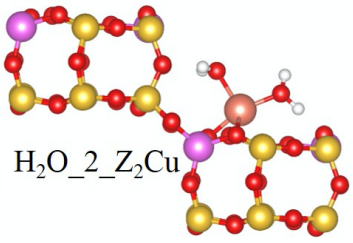

$N_{population} = 2$

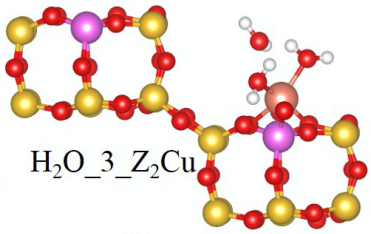

$N_{population} = 2$

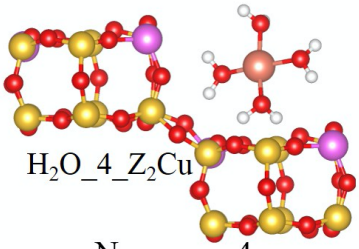

$N_{population} = 4$

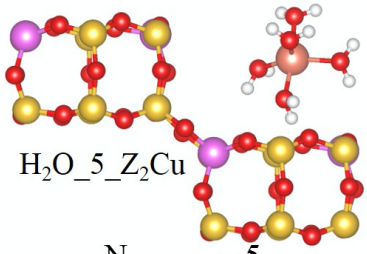

$N_{population} = 5$

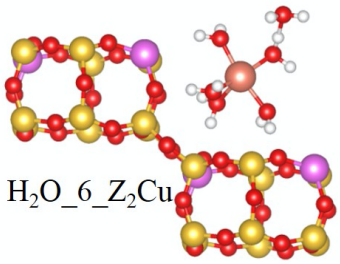

$N_{population} = 5$

NH_3 on Z_2Cu

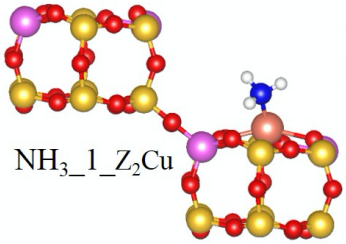

$N_{population} = 1$

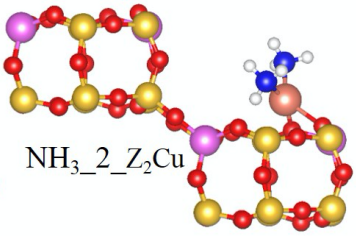

$N_{population} = 2$

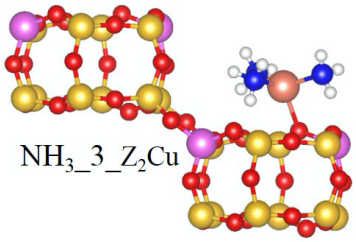

$N_{population} = 3$

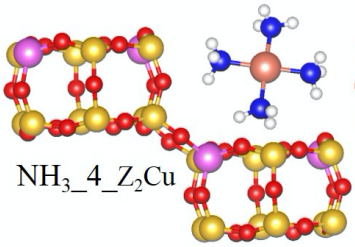

$N_{population} = 4$

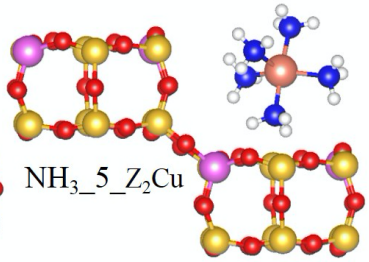

$N_{population} = 5$

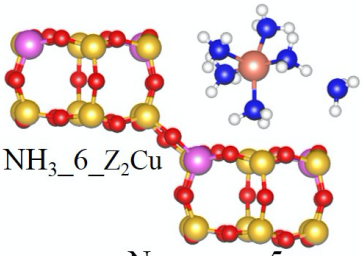

$N_{population} = 5$

H_2O on ZCuOH

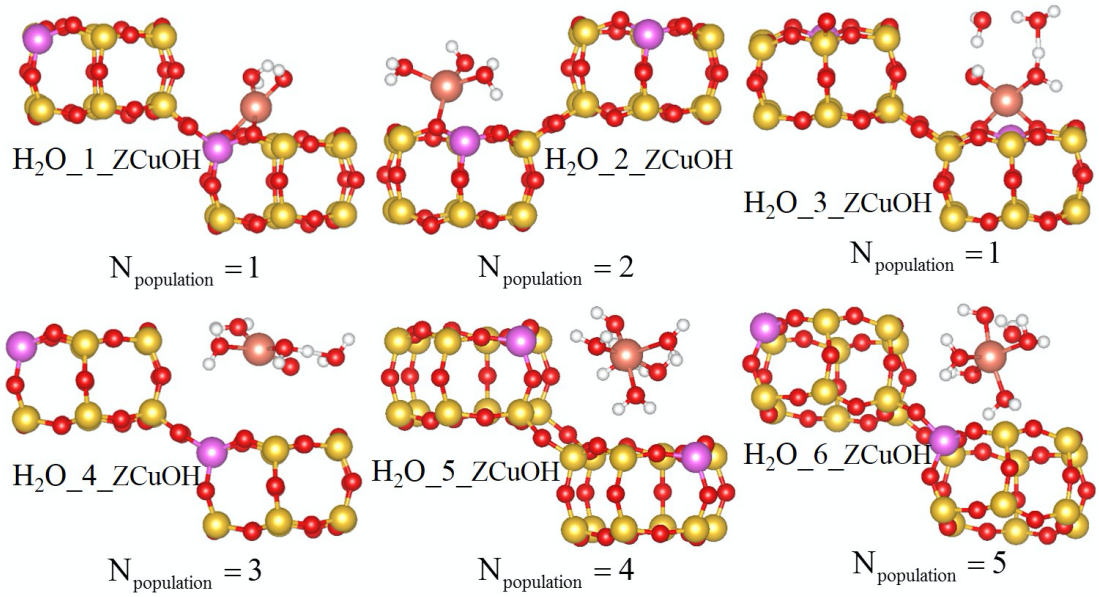

NH_3 on ZCuOH

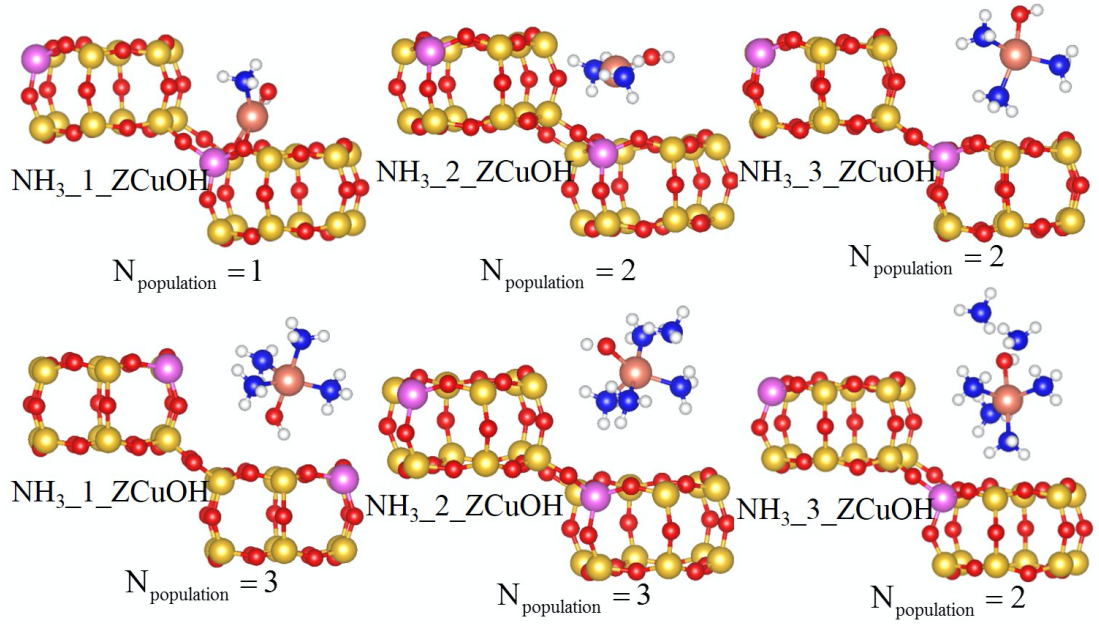

Figure S1. Optimized structures of multiple NH_3 and H_2O (n=1 to 6) adsorbed on Cu-SSZ-13 (ZCu, HZ_2Cu, Z_2Cu and ZCuOH). Each conformation is denoted as molecule_n_Cu-SSZ-13, such that NH_3_1_ZCu is for 1 NH_3 adsorbed adspecies on a ZCu structure. The population of Cu-O or Cu-N bonds ($N_{population}$) contributed from H_2O or NH_3, respectively, is listed in the bottom of the corresponding structure.

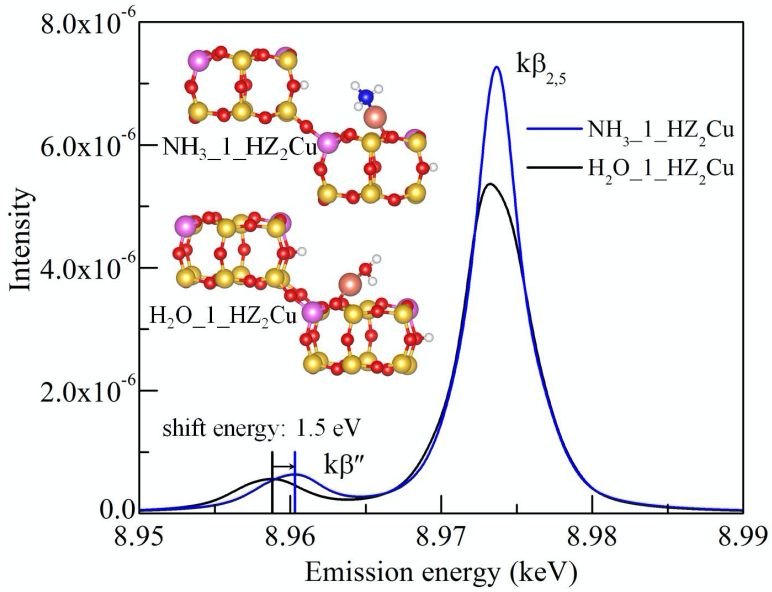

Figure S2. Computational vtc-XES of Cu ions in H_2O_1_HZ_2Cu and NH_3_1_HZ_2Cu. Two emission lines, kβ" and $k\beta_{2,5}$, are presented. The insert displays structures of H_2O_1_HZ_2Cu and NH_3_1_HZ_2Cu.

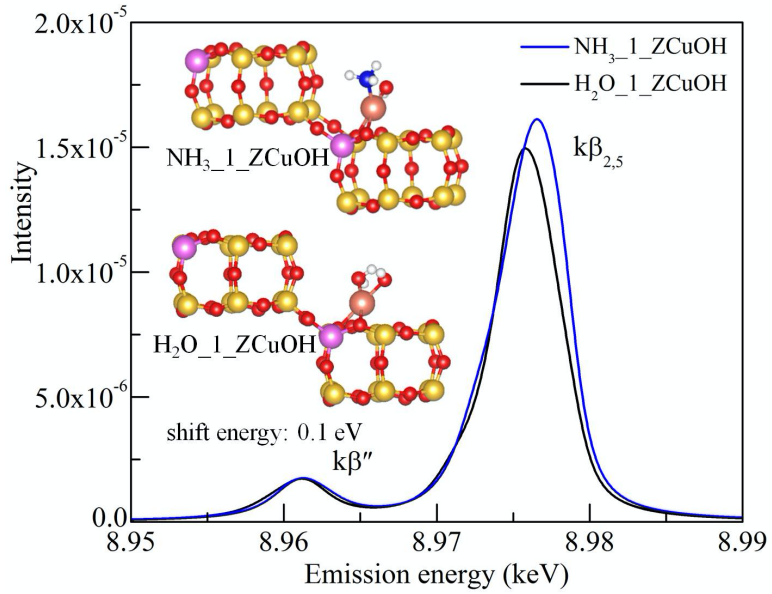

Figure S3. Computational vtc-XES of Cu ions in H_2O_1_ZCuOH and NH_3_1_ZCuOH. Two emission lines, kβ" and $k\beta_{2,5}$, are presented. The insert displays structures of H_2O_1_ZCuOH and NH_3_1_ZCuOH.

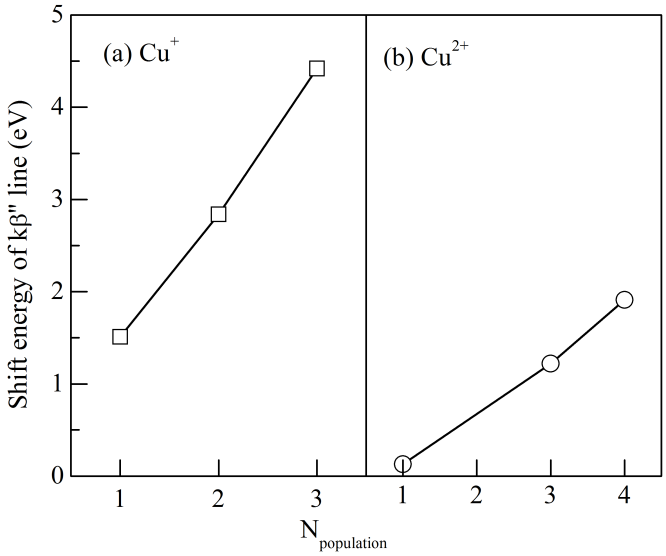

Figure S4. The shift energy of kβ″ line as function of $N_{population}$ for (a) Cu^{+} ion in HZ_2Cu and (b) Cu^{2+} ion in ZCuOH.